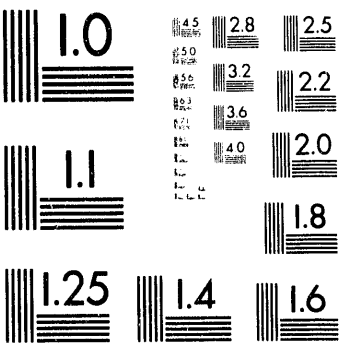
1.0
1.1
1.25
1.4
1.6
1.8
2.0
2.2
2.5
2.8
3.2
3.6
4.0
4.5
5.0
5.6
6.3
7.1
8.0
9.0
10.0

1 of 1

LA-UR-93-1056
N-6-93-R113

Los Alamos National Laboratory is operated by the University of California for the United States Department of Energy under contract W-7405-ENG-36

TITLE: LIQUID RESUPPLY EFFECTS IN MACROLAYER-CONTROLLED NUCLEATE BOILING

AUTHOR(S): Pratap Sadasivan
Cetin Unal
Ralph A. Nelson

SUBMITTED TO: 1993 ASME Winter Annual Meeting
November 28–December 3, 1993
New Orleans, Louisiana

DISCLAIMER

Los Alamos
Los Alamos National Laboratory
Los Alamos, New Mexico 87545

LIQUID RESUPPLY EFFECTS IN MACROLAYER-CONTROLLED NUCLEATE BOILING

by

Pratap Sadasivan, Cetin Unal, and Ralph Nelson

Los Alamos National Laboratory
Nuclear Technology and Engineering Division
Engineering and Safety Analysis Group
Los Alamos, NM 87545

ABSTRACT

Previous studies of the high-heat-flux nucleate boiling regime have made widely varying assumptions about the state of the macrolayer at the beginning of the hovering period of the mushroom bubbles overlying the macrolayer. The uncertainty in the initial state of the macrolayer is largely because little is known about the nature of liquid resupply to the near-heater area following the departure of the mushroom bubble. An assessment of the effect of the differences in liquid resupply mechanisms by experimental means is extremely difficult because of the microscopic length and time scales involved. The present study investigates this using numerical means. A transient three-dimensional computer program was developed and used to simulate various possible resupply mechanisms and consequently different possible initial temperature profiles in the macrolayer. The results show that in commonly used heater materials such as copper, the initial temperature profile in the macrolayer has very little effect on the boiling curve (surface- and time-averaged heat flux and temperature). For higher average surface temperatures observed for low-thermal-conductivity heater materials such as nickel, the boiling curve could shift by a few degrees depending on the initial thermal profile in the macrolayer. Initial thickness of the macrolayer does have an effect on the boiling curve for small values of initial thickness; however, for large initial thicknesses, the effect on the boiling curve is small. It also is shown that changes in the time elapsed between replenishment of the macrolayer (hovering period) do not affect the boiling curve significantly as long as localized dryout of the macrolayer does not occur.

NOMENCLATURE

A_h, A_v	Area of heater, area of vapor stems (m^2)
C_p	Specific heat (J/kg K)

h_{fg}	Latent heat of vaporization (J/kg)
k	Thermal conductivity (W/m K)
L_i	Length of triple-phase contact line for cell i (m)
m_e	Triple-line evaporation coefficient (J/kg m °C)
q'''	Volumetric heat generation (W/m^3)
q, q''	Heat flux (W/m^2)
T	Temperature (K)
t	Time (s)
T_{sat}	Saturation temperature (K)
V	Volume (m^3)
x	Spatial coordinate (m)
ρ_f, ρ_g	Liquid and vapor densities (kg/m^3)
σ	Surface tension (N/m)
τ, τ_1, τ_2	Hovering periods (s)

INTRODUCTION

The high-heat-flux nucleate boiling regime is characterized by the existence of a liquid-rich layer on the heater surface. This so-called macrolayer is interspersed with numerous vapor stems that are anchored to the heater surface. The vapor stems feed into one or more overlying vapor masses attached to the top surface of the macrolayer. Based on systematic photographic studies of the process, Katto and Yokoya (1976) noted that the overlying vapor mushroom bubble grows for a certain period of time while still attached to the macrolayer. The growth is sustained by additional vapor generated by evaporation of the macrolayer. During this growth period, or hovering period, the macrolayer is not replenished with fresh liquid. Therefore, the macrolayer thickness decreases continuously during the course of a hovering period. As the mushroom bubble departs the macrolayer surface at the end of the hovering period, fresh liquid is supplied to the near-surface region and the macrolayer is restored to its initial thickness. Several studies since the early 1980s have related the occurrence of the critical heat flux (CHF) to phenomena associated with the macrolayer, such as the macrolayer conduction, and dryout.

Although the existence of the macrolayer has been demonstrated by several investigators, the role of the macrolayer in the overall process of heat dissipation from the heater surface remains unclear. Several studies reported in the literature have modeled the heat-transfer process in the macrolayer. Salient features of some of these studies are discussed briefly in the next section.

PREVIOUS STUDIES OF MACROLAYER HEAT TRANSFER

Phenomenological models of the high-heat-flux nucleate boiling heat transfer and CHF have been proposed by several investigators. Bhat et al. (1983), Prasad et al. (1985), and Jairajpuri and Saini (1991) presented one-dimensional transient analyses of the macrolayer-controlled heat transfer. Chyu (1987) proposed a mechanism wherein the dominant heat-transfer mode was the evaporation of a microlayer under each vapor stem. Dhir and Liaw (1989) presented a two-dimensional steady-state analysis of nucleate boiling heat transfer. A review of these models was provided by Pasamehmetoglu et al. (1993). In that paper, they presented a new model of macrolayer-controlled heat transfer. They solved the transient conduction equations for the coupled macrolayer-heater domain and found that the dominant heat dissipation component is the evaporation at the triple-interface contact line. As noted by Wayner et al. (1976), heat transfer at the triple-interface contact line occurs as a result of meniscus evaporation and results in extremely high localized heat fluxes in this region. Pasamehmetoglu et al. (1993) modeled this using a lumped approach and represented the meniscus evaporation using a "triple-point coefficient," m_e.

ROLE OF LIQUID RESUPPLY TO THE NEAR-SURFACE REGION

Despite the availability of limited experimental data on the thickness of the macrolayer, there is currently little information available on its other characteristics and their effects on CHF. The liquid resupply mechanism is a key distinguishing factor among all the various approaches that have been used to model CHF.

The hydrodynamic CHF model of Zuber (1958) focuses attention on a structure of large vapor columns above the heater. These columns are assumed to feed into large vapor bubbles above them. The implication is that although a macrolayer may exist on the heater surface, there is sufficient space between the large vapor columns above it that fresh liquid is able to reach the macrolayer continuously. This continuous replenishment of the macrolayer makes it an invariant feature during the boiling process, rendering it irrelevant to the mechanism controlling the CHF. However, several subsequent experimental studies have confirmed that localized dryout of the macrolayer can occur. This suggests that the scenario of continuous replenishment of the macrolayer is unlikely.

However, the surface-controlled CHF model of Haramura and Katto (1983) assumes that the large vapor bubbles are fed directly from the macrolayer; therefore, because the vapor

mushrooms are packed very closely at high heat fluxes, liquid replenishes the macrolayer only intermittently—when one or more vapor bubbles depart the macrolayer. This model suggests that CHF occurs when the macrolayer evaporates before fresh liquid is resupplied to the near-surface region. Thus, the macrolayer plays a significant role in controlling the CHF.

In previous one-dimensional studies of macrolayer-controlled heat transfer, calculations were made for a single hovering period. The assumption was that the heater surface temperature was constant and that the temperature of the macrolayer at the beginning of the hovering period was uniformly equal to the wall temperature. They presented results that showed that heat conduction across the macrolayer was the major component of the overall heat dissipation from the heater surface.

The assumption that the initial temperature of the macrolayer is uniformly equal to the wall temperature is implausible. When fresh liquid is supplied from the bulk liquid to the near-surface upon departure of a mushroom bubble, it is at saturation temperature. The waiting period between liquid replenishment and the beginning of growth of the succeeding mushroom bubble is very small (on the order of a few milliseconds). A simple calculation will show that heating the macrolayer from saturation to the wall temperature (an increase on the order of 10 degrees or more) over such a small time period will require heat-flux levels considerably higher than are imposed on the heater. Thus, the assumption that the macrolayer is initially at a temperature equal to the wall temperature is physically unrealistic.

The two-dimensional steady-state model of Dhir and Liaw (1987) ignores the effect of a periodic resupply of liquid by assuming that the thermal layer is in a steady state. However, the experimental measurements of Yu and Mesler (1977) showing periodic drops in the heater surface temperature suggest that the resupply of liquid to the heater surface does disturb the entire liquid layer. Whether this causes the entire superheated liquid from the previous period to be washed away completely or whether some mixing occurs is an issue that needs to be resolved.

The process of macrolayer replenishment also is affected by the hovering period of the mushroom because replenishment occurs only between hovering periods. Katto and Yokoya (1976) noted that in cases where there is only one vapor bubble or mushroom over the macrolayer at any time, they are not always of the same type. They noted a sequence of three types of mushrooms, and only the first type was spherical. The other types of bubbles were observed to be affected by the wake of the preceding bubble leading to distorted shapes. As a result, the hovering periods were found to be different. Also, there are likely to be multiple

mushroom bubbles over the macrolayer at any given time on larger heaters. This will, in effect, introduce a higher degree of irregularity in the sequence of multiple hovering periods.

The process of liquid resupply to the near-surface region following departure of a vapor mushroom and how this sets the temperature of the newly established macrolayer is as yet unclear. Different phenomenological models of macrolayer heat transfer mentioned in the previous section made widely varying assumptions regarding the liquid resupply process and the resulting temperature of the macrolayer at the start of each hovering period.

The present study is aimed at shedding light on the role of liquid resupply to the heater surface in determining the boiling curve. Resupply of liquid to the heater surface following the departure of vapor mushroom bubbles from the top surface of the macrolayer can be investigated from two aspects: the initial state (thickness and temperature) of the macrolayer after it is reformed and the effect of time elapsed between successive replenishments of the macrolayer. This study presents results on both these effects.

HEAT-TRANSFER MODEL

The model presented by Pasamehmetoglu et al. (1993) has been used in the present study. A heater-macrolayer configuration with a single vapor stem was used and is shown in Fig. 1. Although the particular geometry used to obtain the results presented here is essentially two-dimensional (concentric circles with no azimuthal variations), a three-dimensional code, MACRO3D, has been used for the analysis. The code was developed to examine various three-dimensional aspects of macrolayer-controlled heat transfer.

The heat dissipation from the heater is made up of two components—transient transport into the macrolayer and heat transfer as a result of meniscus evaporation at the triple-line interface of the vapor stems with the liquid and the heater surface. Depending on the state of the macrolayer, transient transport of energy into the macrolayer may result in evaporation at the macrolayer top surface and on the walls of the vapor stems. The effect of the triple-line evaporation is represented by a coefficient, the value of which was obtained indirectly. The coefficient was obtained by tuning it such that the calculated values of surface- and time-averaged heater surface temperature at a given heat flux matched the corresponding experimentally measured surface temperature.

A constant heat flux is imposed on the lower surface of the heater. The top surface of the macrolayer and the wall of the vapor stem are assumed to be at saturation temperature during the entire process. The heat transfer from meniscus evaporation is represented as a heat-loss boundary condition along the periphery of the base of the vapor stems. Unlike in previous analyses discussed in the Introduction, no stringent assumption is made here concerning the initial temperature distribution in the heater. Instead, we start with a reasonable but arbitrary initial temperature distribution in the heater. The temperature distribution in the macrolayer at the beginning of each hovering period is specified depending on the particular mechanism of replenishment being investigated. With these initial conditions, the energy equation is solved for the combined heater-macrolayer domain for successive hovering periods allowing the heater temperature distribution to evolve to its desired state. The surface- and time-averaged (STA) heater surface temperature and surface flux are calculated at the end of each hovering period, and stationary conditions are reached when the STA values in one period are within a specified tolerance level of those calculated for the preceding period. The choice of initial temperature distribution in the heater does not affect the overall results in STA values; it does have an effect on the number of hovering period calculations required to reach the stationary state.

Computer Program

The present calculations were carried out using a three-dimensional transient heat conduction analysis code, MACRO3D. Complete details on this code are provided by Sadasivan et al. (1993). The salient features of the code are outlined below.

MACRO3D uses a three-dimensional control volume discretization scheme to represent the solution domain—the composite structure composed of the heater and the liquid macrolayer. The algebraic equations used to represent the system are obtained by carrying out energy balances on each individual control volume.

The control volumes have polygonal cross sections (in the radial plane) and have vertical faces in the axial plane. The polygons could be regular hexagons or a set of irregular polygons. A sample element configuration is shown in Fig. 2. The polygonal mesh is obtained by generating a series of points within the problem domain area and then carrying out a Voronoi tessellation on these points.

For purposes of evaluating diffusive flows across the face of each control volume, the system parameters are assigned to the center of each control volume and the internodal distance is used as the characteristic length across which diffusion occurs. This is facilitated because the mesh

generation procedure is such that the common face between two control volumes across which diffusion takes place is normal to the line that connects their centers.

Governing Equations

The basis of the solution is the differential form of the conservation of energy:

$$\text{Div (k grad T)} + q''' = \frac{\partial}{\partial t}(\rho\, C_p\, T) \ . \tag{1}$$

One can obtain a lumped-parameter approximation to Eq. (1) for the temperature at any node as

$$\sum_i A_i\, k_i \frac{\Delta T_i}{\Delta x_i} + V_j\, q_j''' = V_j\, \rho_j\, C_{pj} \frac{\partial T_j}{\partial t} \ , \tag{2}$$

where the subscript j refers to the node under consideration and subscript i refers to the lumped quantities in each of the neighboring elements of node j. Δx_i is the distance between the center of node j and that of its neighboring element i. The geometry of the grid structure is sketched in Fig. 3. If node j has n_j coplanar neighbors, and two axial neighbors, Eq. (2) can be written as

$$V_j\, \rho_j\, C_{pj} \frac{T_j^{n+1} - T_j^n}{\Delta t} = \sum_{i=1}^{n_j+2} A_i k_i \frac{T_i - T_j}{\Delta x_i} + q''' V_j \ , \tag{3}$$

where the second term on the right-hand side is a source term that accounts for the internal generation (assumed to be zero in the present case) and the boundary conditions. Under a semi-implicit scheme, the right-hand side of Eq. (3) would be the average of its values evaluated at the current and previous time steps.

The boundary conditions are included in the energy balance statement for each element [Eq. (3)] by representing them as additional volumetric heat source terms. Thus, if element j is subjected to an external heat flux, q''_j, on it face of area A_j, we represent this heat input as a volumetric heat source term as

$$q''' = \frac{q''_j\, A_j}{V_j} \ . \tag{4}$$

Similarly, if one face of cell j is maintained at a constant temperature T_{sat}, we can represent this as an additional heat-source term in cell j, arising from conduction from an artificial neighboring cell on that face at a constant temperature of T_{sat}. This term can be written as

$$q''' = \frac{k_j A_j (T_{sat} - T_j)}{V_j} \quad . \tag{5}$$

The triple-phase contact line at the base of the vapor stems dissipates heat by continuous evaporation of the meniscus. As we mentioned previously, the heat transfer by meniscus evaporation is represented by an adjustable coefficient, m_e, following the approach of Pasamehmetoglu et al. (1993). The energy dissipated by meniscus evaporation at the base of a vapor stem is represented by

$$Q_{meniscus} = m_e \ (L_i) \ (h_{fg}) \ (T_i - T_{sat}) \ , \tag{6}$$

where L_i is the length of the triple interphase line for control volume i. Equation (6) can be written in volumetric terms as

$$q''' = \frac{m_e \ (L_i) \ (h_{fg}) \ (T_i - T_{sat})}{V} \quad . \tag{7}$$

This energy dissipation is assumed to be concentrated in a small region of the heater surface at the base of the stem along its periphery. The remaining area of the vapor contact area on the heater surface is assumed to be adiabatic.

The interface between the heater and liquid/vapor is a common face for the control volumes that are located on either side of it such that each control volume is made up of a homogeneous material. The presence of liquid on one side of the interface and solid heater material on the other side implies a substantial discontinuity in the diffusion coefficient across the interface. The harmonic mean approach suggested by Patankar (1980) has been used to prescribe the effective diffusion coefficient across the interface.

The set of equations (3) written for each cell comprises a large, sparse linear system of equations. This system is solved at each time step using the Conjugate Gradient Squared (CGS) algorithm. A highly vectorized version of the solver routine has been adapted from Rider et al. (1991).

RESULTS

The MACRO3D computer code has been used to investigate the effects of liquid resupply—the temperature profile in the macrolayer at the beginning of each period, the thickness of the macrolayer following replenishment, and the time elapsed between successive replenishments of the macrolayer. The results are presented below.

Macrolayer State at the Beginning of a Hovering Period

In the first set of calculations, the effect of the initial condition of the macrolayer on the STA heat flux and temperature was investigated. The true state in the macrolayer is unknown, and experimental resolution of the temperatures in such a small region is an extremely formidable task. In the present study, our objective is to determine the relative sensitivity of the STA surface temperatures and heat fluxes to various initial temperature profiles in the macrolayer. As mentioned earlier, it is not realistic to assume that the macrolayer attains the wall temperature at the beginning of the period. If the macrolayer has not dried out completely during a hovering period, there will be a layer of superheated liquid on the heater surface (the thickness of this "residual layer" will be the initial thickness of the macrolayer minus the amount evaporated during the period). There are several possible temperature distributions in the macrolayer when it is reestablished at the end of each hovering period. The simplest scenario is that the entire superheated residual macrolayer is washed away by the replenishing liquid from the bulk, and thus, the new macrolayer is made up entirely of saturated liquid. This is the approach used in the model of Pasamehmetoglu et al. (1993). On the other hand, if the residual macrolayer is not washed away, it could simply be mixed with makeup saturated liquid. In this "mixing cup" case, the entire macrolayer at the beginning of the next period will be at a uniform temperature, higher than the saturation value.

Another possible scenario is that all or part of the residual superheated liquid macrolayer remains intact and the amount of liquid required to restore the thickness to the initial value is made up with saturated liquid from the bulk. In the present study, this scenario has been investigated with different values assigned to the percentage of the residual macrolayer that remains undisturbed. The various possible macrolayer initial temperature profiles are shown schematically in Fig. 4.

The configuration used in the present study is shown in Fig. 1. A single "average" stem of radius 0.085 mm is assumed to be located concentrically on a heater of radius 0.595 mm. The void ratio is about 2.0%. The triple-point coefficient, m_e, is set to 280×10^{-6} kg/m s °C. The reader is referred to Pasamehmetoglu et al. (1993) for a discussion of this configuration.

The heat flux imposed is 1.075 MW/m^2. There is at present no completely reliable expression available in the literature for the initial macrolayer thickness. Haramura and Katto (1984) proposed

$$\delta_i = \frac{\pi}{2}\,\sigma\left(\frac{\rho_f + \rho_g}{\rho_i\,\rho_g}\right)\left(\frac{A_v}{A_h}\right)^2\left(\frac{\rho_g\ h_{fg}}{q}\right)^2, \tag{8}$$

but the premise of this equation—that the macrolayer thickness is determined by the Helmholtz instability on the vapor stem walls—is not entirely supported by experiments. Rajvanshi et al. (1992) obtained experimental measurements of macrolayer thickness in the vapor mushroom region of nucleate boiling (interference region) and noted that the experimental values of the macrolayer thicknesses were approximately twice those predicted by the above equation. However, Eq. (8) has been used in the present study of liquid resupply effects to obtain conservative estimates. The hovering period was determined using the expression of Haramura and Katto (1984):

$$\tau_d = \left(\frac{3}{4\,\pi}\right)^{1/5}\left[\frac{4\,(\frac{11}{16}\rho_f + \rho_g)}{g\,(\rho_f - \rho_g)}\right]^{3/5}\left[\frac{A_h\,q}{\rho_g\,h_{fg}}\right]^{1/5}. \tag{9}$$

For the conditions of these calculations, Eqs. (8) and (9) predict an initial macrolayer thickness of 98 μm and a hovering period of 50.589 ms, respectively. Table I shows the results of the calculations.

For the case when the entire residual superheated macrolayer is washed away by the oncoming liquid from the bulk (point 1), the new macrolayer is uniformly at the saturation temperature. For this base point, the STA temperature was found to be 389.8 K for copper. Point 2 is the case when the residual macrolayer is allowed to mix completely with makeup saturated liquid. In this case, the new macrolayer at the beginning of the hovering period is still at a uniform temperature but several degrees higher than the saturation value. Copper's STA surface temperature for this case was 390.2 K. In both these cases, the heater surface temperatures at the beginning of each period were dropped instantaneously to account for the fact that reestablishment of the entire macrolayer causes a rapid cooling of the heater surface as observed by Yu and Mesler (1977). Henceforth, we will call the rapid cooling a "quench."

Points 3 and 4 in Table I are cases where part, or all, of the residual macrolayer was allowed to remain on the heater surface under the assumption that the oncoming liquid from the bulk of the pool does not disturb the entire residual macrolayer. In these cases, quenching of the heater surface does not occur. The highest STA surface temperature is, as expected, obtained for the case when the entire residual macrolayer remains intact. The maximum STA temperature for copper is 390.4 K and is only 0.6 K higher than the case where the entire residual macrolayer is washed away.

The role of the surface quench at the beginning of each period, which was observed experimentally by Yu and Mesler, is seen to have only a small effect on the STA temperatures for copper. Table I also shows the results obtained for the same calculations carried out on lower conductivity heater materials--aluminum and nickel. The configuration used for these calculations is the same as that described earlier for copper. This essentially assumes that the site density and the triple-point coefficient are the same for all materials. This assumption is reasonable for purposes of identifying the specific effect of a change in the heater thermal properties. The results of Table I are shown graphically in Fig. 5. It is clear from the figure that the effect of changes in initial temperature profiles increases as the heater thermal conductivity decreases. The relative contributions of transient transport and meniscus evaporation for the three heater materials are shown in Fig. 6. The dashed lines correspond to row 1 in Table I, and the solid lines correspond to row 4. As the thermal conductivity of the heater decreases, the relative contribution of transient transport increases, and the STA temperature increases at the same time. As shown in Table I and Fig. 5, the effects of initial temperature profile, and therefore those of the liquid resupply process, become greater when the heater thermal conductivity decreases. However, this could be the result of the increased role of transient transport or of the increase in STA temperature itself. This will be addressed later in this section.

The transient variation of surface-averaged temperatures during the converged hovering period for various liquid resupply conditions is shown in Fig. 7 for a copper heater. In cases where all or part of the residual macrolayer from the previous hovering period remains intact on the heater surface, the temporal variation of the surface-averaged temperatures during the converged hovering period is relatively small. The range between the maximum and minimum surface-averaged temperature during the period is on the order of 0.1°C. This range decreases as more and more of the residual macrolayer remains intact. In cases where the residual macrolayer is either washed away completely or mixed with makeup liquid, the surface is quenched instantaneously to a lower temperature at the beginning of the period, and consequently the temporal variation in the instantaneous surface-averaged temperature is higher—and can be as

high as 1.5°C. This value is of the same order as that observed in the experiments of Yu and Mesler (1977) and suggests that the actual liquid resupply process does indeed disturb the entire residual macrolayer.

The above results indicate that changes in the initial temperature distribution as a result of changes in liquid resupply conditions have only a small effect on the STA surface temperature in common experimental heater materials such as copper. The instantaneous quench that occurs in cases where the residual macrolayer is washed away completely at the end of each period causes a small temporal variation in the surface-averaged temperature during the hovering period. For less-conducting heater materials such as nickel, the boiling curve could shift by a few degrees, depending on the temperature profile in the macrolayer.

Figure 8 shows the influence of initial macrolayer thickness on the resulting converged STA surface temperatures. The sensitivity of the STA temperatures to the initial macrolayer thicknesses is small for high initial thicknesses, but the STA temperatures become more sensitive to changes in thickness as the initial thickness is reduced. The STA temperatures decrease continuously with decreasing initial thicknesses up to a certain point. For the larger thicknesses, the thermal resistance to conduction is relatively high, and the dominant component of heat dissipation is meniscus evaporation. Thus, the conduction through the macrolayer is unimportant and macrolayer thickness is not a major factor. However, as the initial thickness is reduced to lower values, transient conduction through the macrolayer increases and the STA surface temperature decreases. As the initial thickness is reduced further, the STA temperatures begin to increase because the macrolayer dries out completely during each period, and thus the heater surface is in effect insulated for a portion of each period.

We also repeated some of the calculations of Table I using a lower value of initial macrolayer thickness. For a copper heater and an initial thickness of 49 μm, the STA temperature for the case when the entire residual macrolayer is washed away is 387.6 K. The corresponding value for the case when the entire residual macrolayer remains intact on the surface is 387.8 K. These results are also shown in Fig. 5 (curve labeled 4). Although the relative importance of transient conduction is higher as the initial thickness is decreased, the effect of macrolayer temperature profile is diminished. In our discussion of Fig. 6, the increased sensitivity of the STA surface temperatures to changes in macrolayer thermal profile was attributed to either the increased importance of transient transport or the increase in the STA temperature itself. The present results suggest that the influence of changes in liquid resupply conditions is related directly to the STA temperature and not to the relative importance of transient transport.

Effect of Multiple Hovering Periods

As we noted earlier, Katto and Yokoya (1976) observed that successive mushroom bubbles departing the macrolayer could do so at different frequencies. In their experiments, they observed three kinds of mushroom bubbles. The first type of bubbles were approximately spherical upon departure, but the other two had distorted shapes. They found that the hovering periods for the second and third type of bubbles were less than those of the first type of bubbles. Figure 9 shows their data. Haramura and Katto (1984) proposed Eq. (9) for evaluating the hovering period of the spherical bubbles.

All the analyses of the macrolayer heat transfer that were discussed earlier have considered a single hovering period or cycle time. Multiple hovering periods such as those observed by Katto and Yokoya suggest that re-establishment of the macrolayer occurs at varying frequencies. The influence of such a variation on the overall STA surface temperatures is not yet clear. In the second part of the present study, we explored this issue by allowing the length of the hovering period to change in a prespecified manner from one period to the next.

Calculations were carried out for a copper heater with a heat flux of 1.075 MW/m^2 and an initial macrolayer thickness of 98 μm for a case with a sequence of two different hovering periods. The length of the first period, τ_1, in each sequence is 50.589 ms [value predicted by Eq. (9)] and that of the second, τ_2, is 25.295 ms. The multiplicity of periods causes a very small periodic variation in the surface- and period-averaged temperature and heat flux. Under conditions of stationarity, the surface- and period-averaged heat flux is 1.063 MW/m^2 for τ_1 and 1.096 MW/m^2 for τ_2. Similarly, the surface- and period-averaged temperature is 389.7 K for τ_1 and 389.6 K for τ_2. The surface- and period sequence-averaged temperature, 389.7 K, is very close to the corresponding value, 389.8 K, for the case when the length of all hovering periods was uniform at 50.589 ms.

For the case of τ_1 = 50.589 ms and τ_2 = 10.118 ms, the surface- and period-averaged temperature and heat flux vary to a higher degree between τ_1 and τ_2 than in the case of τ_1 = 50.589 ms and τ_2 = 25.295 ms. Under conditions of stationarity, the surface- and period-averaged heat flux is 1.055 MW/m^2 for τ_1 and 1.184 MW/m^2 for τ_2. Similarly the surface- and period-averaged temperature is 389.6 K for τ_1 and 389.4 K for τ_2. However, the temperature values averaged over the sequence of periods, 389.5 K, is very close to the value of 389.8 K, for the case when all periods were uniformly equal to 50.589 ms. Similar results were obtained for the case of τ_1 = 101.178 ms and τ_2 = 50.589 ms.

Calculations were repeated for the case of nickel as well. As listed in Table I, for values of $q = 1.075$ MW/m^2, initial macrolayer thickness = 98 μm, $\tau = 50.589$ ms, and $m_e = 280 \times 10^{-6}$ kg/m s °C, the STA heater surface temperature was 415.7 K. When calculations were repeated for multiple periods $\tau_1 = 50.589$ ms and $\tau_2 = 25.295$ ms, the surface- and period-sequence-averaged temperature was calculated to be 414.5 K. As was found in the case of the influence of varying initial temperature profiles in the macrolayer, the influence of multiple hovering periods on the boiling curve is slightly higher for nickel than for copper.

The contribution of the two components to the overall heat transfer for the case $\tau_1 = 50.589$ and $\tau_2 = 25.295$ ms is shown in Fig. 10. It would seem that the insensitivity of the average temperatures to the multiplicity of periods is a result of the domination of the meniscus evaporation component of heat dissipation over the transient transport component. To verify whether this is so, we carried out another set of calculations for an artificial case where the heat flux and initial macrolayer thickness were chosen such that the transient conduction component would dominate for a portion of the longest period in the sequence of multiple periods.

Calculations were made for a heat flux of 1.4 MW/m^2 and an initial macrolayer thickness of 40 μm. For the case when all periods are uniformly equal to 53.379 ms (predicted by the Haramura-Katto equation), the STA surface temperature was 389.4 K. For alternating periods of 53.376 ms and 26.69 ms, the surface- and period-sequence-averaged temperature was 389.7 K, only slightly different from the uniform-period value. The contributions of the two heat-transfer components are shown in Fig. 11. During the longer hovering period in the sequence, the transient conduction component is comparable to the meniscus evaporation component for the last half of the period and the dominant component in heat dissipation for the last 15% of the period. In typical situations where macrolayer dryout does not occur, the transient transport component is the dominant component only for such small fractions of the overall period. Thus, in general, meniscus evaporation is the main component. In such cases, multiplicity of hovering periods does not affect the converged STA heater surface temperatures significantly.

Calculations also were carried out for the case where the hovering period was allowed to vary randomly between 20 ms and 85 ms. This is an approximate simulation of the case where there are multiple vapor mushrooms over the macrolayer at one time. These mushrooms will have different hovering periods. This situation is simulated here by essentially representing the multiple mushroom bubbles by a single "average" mushroom the hovering period of which is allowed to vary in a random manner. The area- and period-averaged surface temperatures varied by a maximum of 1 degree from one period to another, and the value averaged over a window of

several consecutive periods was again found to be close to the value of 389.4 K, obtained for the case when all periods were uniformly equal to 53.379 ms.

These results suggest that in cases where there are multiple hovering periods as observed by Katto and Yokoya (1976), the spherical bubble equation of Haramura and Katto (1984) [Eq. (9)] can be used with no significant loss of accuracy. It should be pointed out that these results are based on calculations where the macrolayer thickness is assumed to be uniform over the heater surface. In cases where there are spatial variations in the macrolayer thicknesses, these conclusions will hold only so far as there is no localized dryout of the macrolayer—that is, for the lower portion of the mushroom bubble boiling region on the boiling curve.

The relative insensitivity of the STA heater surface temperatures to variations in the hovering period is also consistent with experiments that have shown that the low and intermediate nucleate boiling regions are relatively unaffected by changes in gravity, whereas the region close to CHF is sensitive to gravity. The hovering period of the mushrooms decreases as gravity is increased, but the present calculations indicate that this does not have any appreciable effect on the STA surface temperatures as long as the macrolayer does not dry out during any period. This is the case at low and intermediate heat fluxes, where the initial macrolayer thickness is high. However, at heat fluxes close to CHF, the initial macrolayer thickness is lower; consequently, the macrolayer could dry out if the hovering period is sufficiently long. Thus, the STA temperatures become sensitive to the hovering period values and thus to the gravity level.

CONCLUSIONS

The model of Pasamehmetoglu et al. (1993) for the vapor mushroom region of nucleate boiling has been used to investigate various liquid resupply effects on the boiling curve. Differences in initial temperature profile in the macrolayer as a result of changes in resupply conditions do not affect the boiling curve for commonly used heater materials such as copper for which the STA surface temperatures are relatively low. Also, the rapid cooling of the heater surface at the beginning of each period does not affect the STA temperatures significantly. For lower conductivity heater materials such as nickel, the STA temperatures are higher and are more sensitive to the initial temperature profile in the macrolayer. Changes in the boiling curve from one experiment to another on such heater materials may be caused in part by differences in the nature of liquid resupply to the heater surface. Scatter in boiling curve data resulting from changes in resupply conditions will be higher as STA surface temperatures increase. The effect

will be higher as the boiling curve shifts toward higher temperatures as a result of the influence of other parameters such as roughness and wettability.

The initial thickness does affect the boiling curve but only if the thickness is sufficiently small that macrolayer conduction becomes the dominant factor at some time during the hovering period. For relatively high initial thicknesses such as at low heat fluxes, the boiling curve is insensitive to changes in initial thicknesses. At very low initial thicknesses, such as at heat fluxes close to CHF, macrolayer dryout occurs during a hovering period, and consequently, the boiling curve shifts toward higher temperatures as the initial macrolayer thickness is reduced to very low values.

The effect of multiple hovering periods on the boiling curve has been found to be very small regardless of the dominant component of heat dissipation. Therefore, for purposes of macrolayer heat-transfer analysis, multiple periods can be ignored, and calculations can be based on spherical bubble analyses such as that of Haramura and Katto.

REFERENCES

Ball, S.J ., 1976, "ORECA-I: A Digital Computer Code for Simulating the Dynamics of HTGR Cores for Emergency Cooling Analysis," Oak Ridge National Laboratory, ORNL/TM-5159.

Bhat A. M., Prakash, R., and Saini, J. S., 1983, "Heat Transfer in Nucleate Pool Boiling at High Heat Flux," Int. J. Heat Mass Transfer, Vol. 26, pp. 833-840.

Bhat, A. M., Prakash, R., and Saini, J.S ., 1983, "On the Mechanism of Macrolayer Formation in Nucleate Pool Boiling at High Heat Flux," Int. J. Heat Mass Transfer, Vol. 26, pp. 735-740.

Bhat, A. M., Saini, J. S., and Prakash, R., 1986, "Role of Macrolayer Evaporation in Pool Boiling at High Heat Flux," Int. J. Heat Mass Transfer, Vol. 29, pp 1953-1961.

Chappidi, P. R., Unal, C., Pasamehmetoglu, K. O., and Nelson, R. A., 1991, "Development of a Multiple Vapor Stem Model for Saturated Pool Nucleate Boiling at High Heat Fluxes on a Horizontal Surface," Los Alamos National Laboratory report LA-UR-91-1939.

Chyu, M-C., 1987, "Evaporation of Microlayer in Nucleate Boiling Near Burnout," Int. J. Heat Mass Transfer, Vol. 30, pp. 1531-1538.

Gaertner, R. F., 1965, "Photographic Study of Nucleate Boiling on a Horizontal Surface," ASME Journal of Heat Transfer, 87, pp. 17-29.

Haramura, Y., and Katto, Y., 1983, "A New Hydrodynamic Model of Critical Heat Flux, Applicable Widely to Both Pool and Forced Convection Boiling on Submerged Bodies in Saturated Liquids," Int. J. Heat Mass Transfer, 26, pp. 389-399.

Jairajpuri, A. M., and Saini, J. S., 1991, "A New Model for Heat Flow through Macrolayer in Pool Boiling at High Heat Flux," Int. J. Heat Mass Transfer, Vol. 34, pp. 1579-1591.

Katto, Y., and Yokoya, S., 1976, "Behavior of Vapor Mass in Saturated Nucleate and Transition Pool Boiling," Heat Transfer Japanese Research, Vol. 5, pp. 45-65.

Pasamehmetoglu, K. O., and Nelson, R. A., 1991, "Cavity-to-Cavity Interaction in Nucleate Boiling: The Effect of Heat Conduction Within the Heater," AIChE Symp. Ser., 87, n283, pp. 342-351. (also available as Los Alamos National Laboratory document LA-UR-91-165).

Pasamehmetoglu, K. O., Chappidi, P. R., Unal, C., and Nelson, R. A., 1993, "Saturated Pool Nucleate Boiling Mechanisms at High Heat Fluxes," Int. J. Heat Mass Transfer, in press.

Patankar, S. V., 1980, "Numerical Heat Transfer and Fluid Flow," Hemisphere Publishing Company.

Prasad, N. R., Saini, J. S., and Prakash, R., 1985, "The Effect of Heater Wall Thickness on Heat Transfer in Nucleate Pool Boiling at High Heat Flux," Int. J. Heat Mass Transfer, Vol. 28, pp. 1367-1375.

Rajvanshi, A. K., Saini, J. S., and Prakash, R., 1992, "Investigation of Macrolayer Thickness in Nucleate Pool Boiling at High Heat Flux," Int. J. Heat Mass Transfer, Vol. 35, pp. 343-350.

Sadasivan, P., Unal, C., and Nelson, R. A., 1993, "MACRO3D—A Three-Dimensional Finite Volume Computer Code for the Analysis of High Heat Flux Nucleate Boiling," Los Alamos National Laboratory report, in press.

Torikai, K., 1966, "Heat Transfer in a Contact Area of a Boiling Bubble on a Heating Surface," Bull. JSME, Vol. 10, pp. 338-348.

Torikai, K., and Yamazaki, T., 1967, "Dry State in a Contact Area of a Boiling Bubble on a Heating Surface," Bull. JSME, Vol. 10, pp. 349-355.

Wayner, P. C. Jr., Kao, Y. K., and LaCroix, L. V., 1976, "The Interline Heat Transfer Coefficient of an Evaporating Film," Int. J. Heat Mass Transfer, Vol. 19, pp. 487-492.

Yu, C-L., and Mesler, R. B., 1977, "A Study of Nucleate Boiling Near the Peak Heat Flux Through Surface Temperature Measurement," Int. J. Heat Mass Transfer, Vol. 20, pp. 827-840.

TABLE I

CALCULATED VALUES OF STA SURFACE TEMPERATURES FOR DIFFERENT INITIAL TEMPERATURE PROFILES IN THE MACROLAYER

Point	Description of Initial Temperature Profile in the Macrolayer	STA Surface Temperature (K)		
		Copper	Aluminum	Nickel
1	Entire residual macrolayer is washed away and replaced by saturated liquid.	389.8	399.4	415.7
2	Residual macrolayer is mixed completely with saturated liquid.	390.2	400.4	418.4
3	25% of residual macrolayer remains intact, and the remainder is made up with saturated liquid.	390.1	400.3	418.0
4	Entire residual macrolayer remains intact, and the remainder is made up with satuarated liquid.	390.4	401.0	419.5

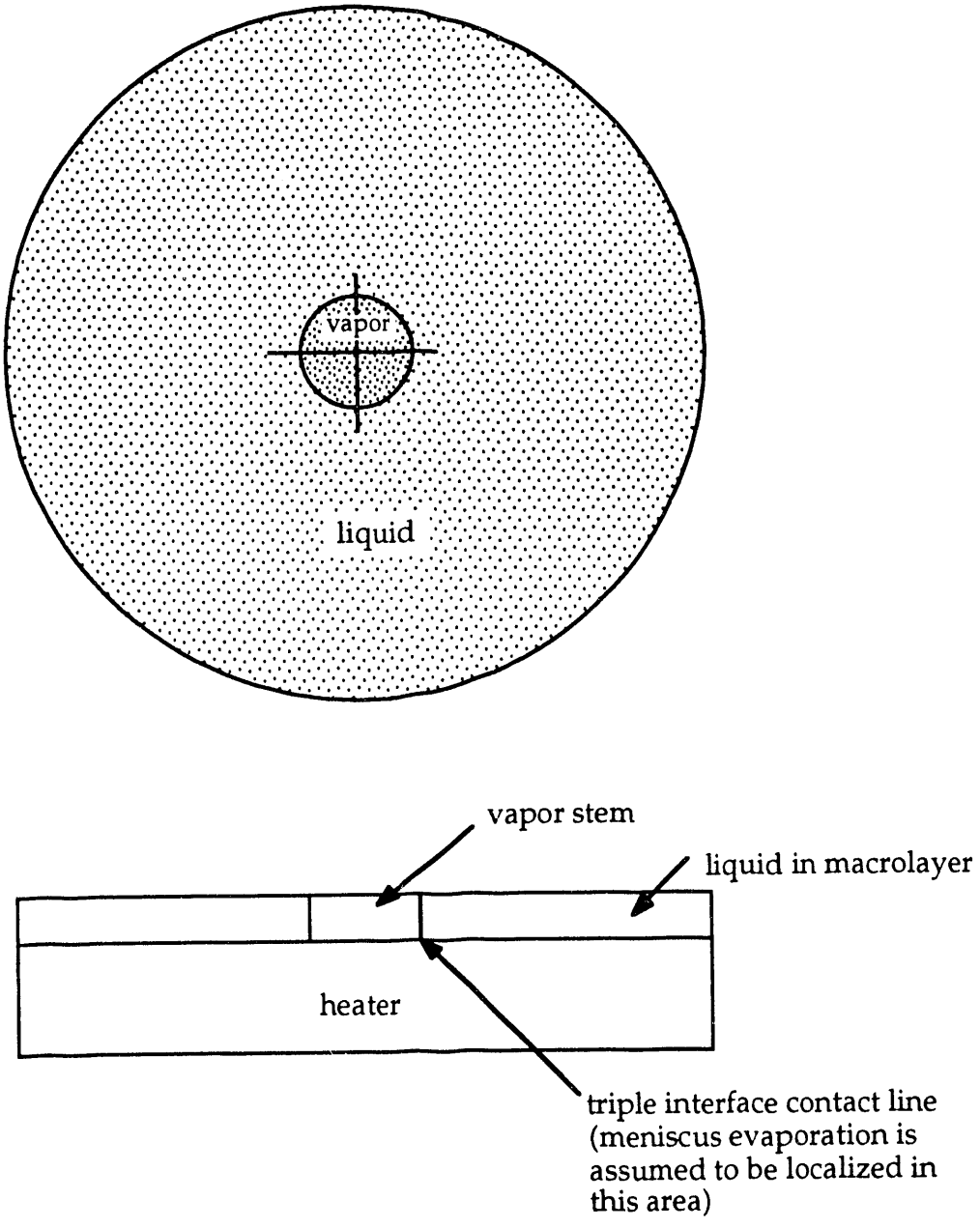

Fig. 1. Configuration of vapor stem, liquid, and heater.
(Heater radius = 0.595 mm, Vapor stem radius = 0.085 mm).

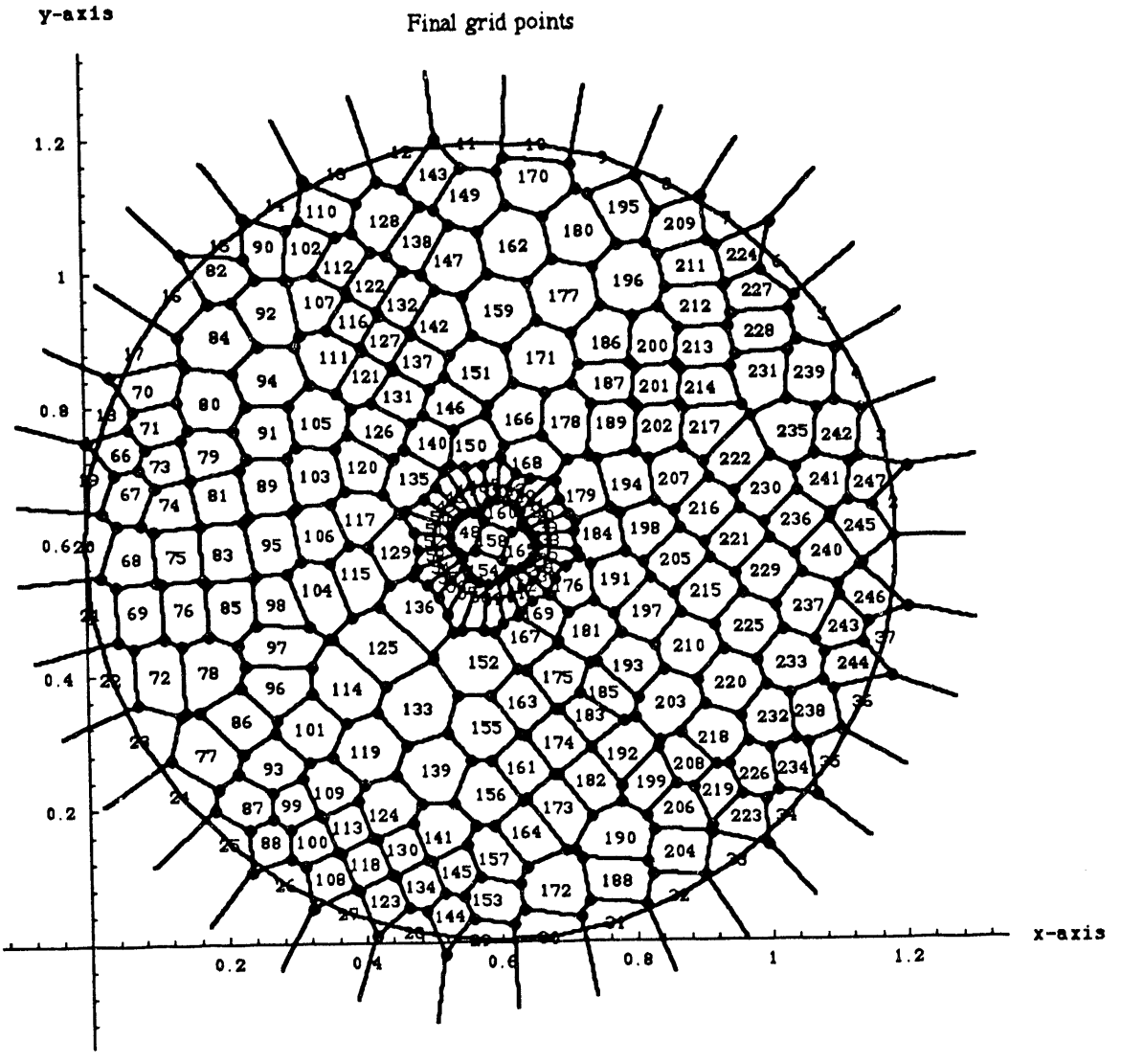

Fig. 2. Example of an irregular mesh scheme used in the calculations.

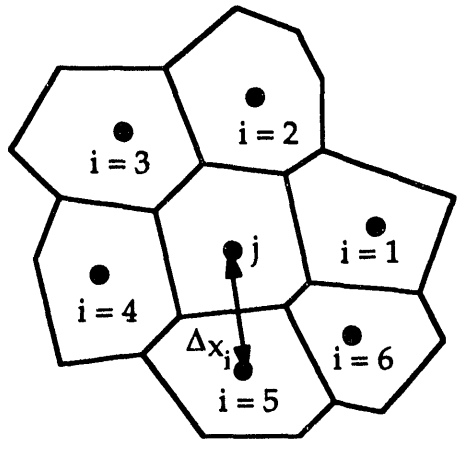

(a)

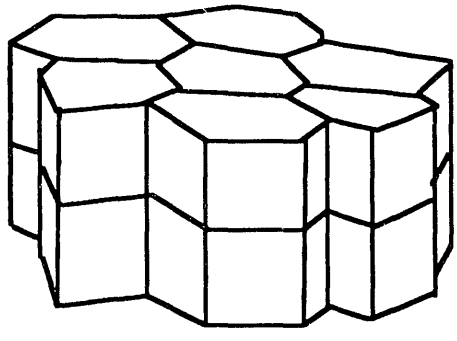

(b)

Fig. 3. Geometry of grid structure shown for an irregular mesh: Cell j with six coplanar neighbors: (a) top view, (b) side view. (Top and bottom faces of each cell are horizontal and side faces are vertical.)

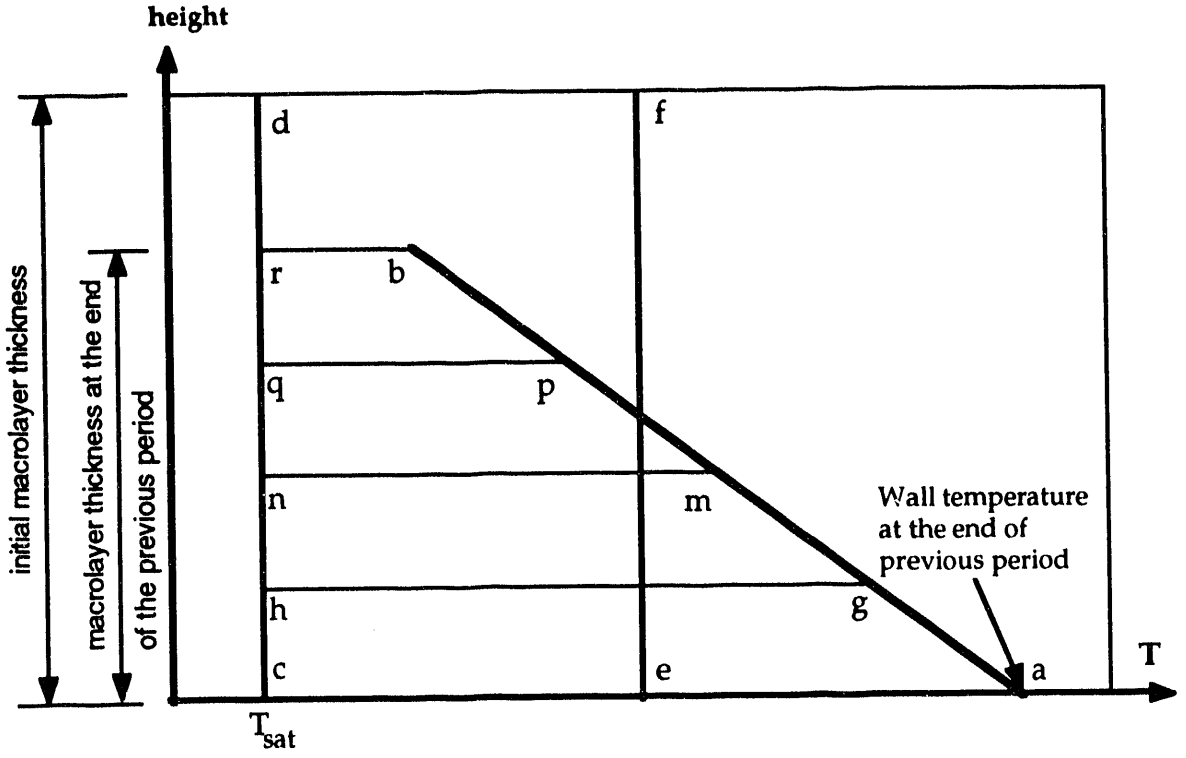

Line abr	Temperature profile in the macrolayer at the end of the previous period.
Line cd	Entire residual macrolayer is washed away and replaced with saturated liquid.
Line ef	Residual macrolayer is mixed with makeup saturated liquid.
Line aghd	25% of residual macrolayer remains intact.
Line amnd	50% of residual macrolayer remains intact.
Line apqd	75% of residual macrolayer remains intact.
Line abrd	Entire residual macrolayer remains intact.

Fig. 4. Examples of initial temperature profiles in macrolayer (for illustrative purposes; not to scale).

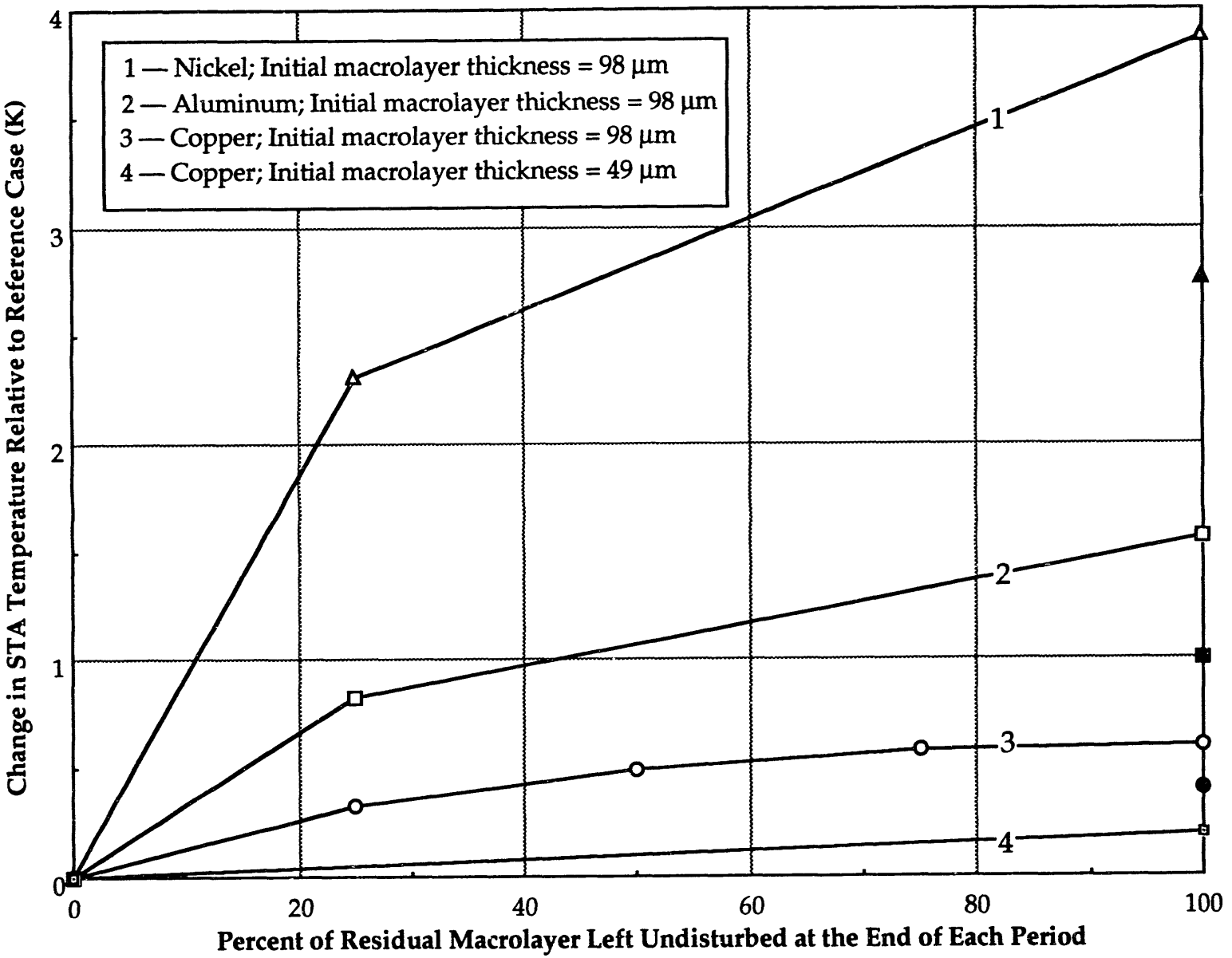

Fig. 5. Effect of change in initial temperature profile on STA temperature. (Solid symbols represent data where residual macrolayer is mixed with saturated makeup liquid).

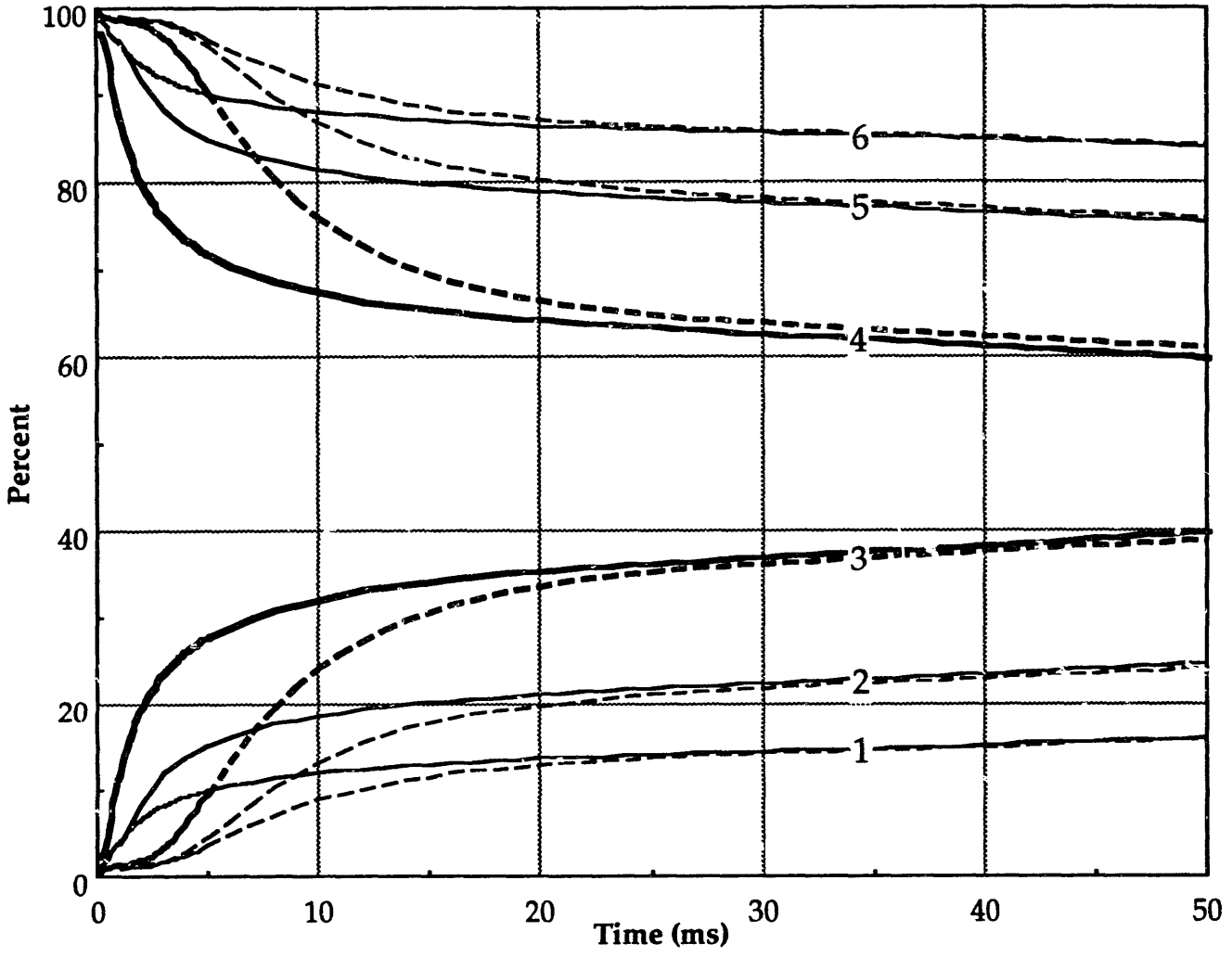

1—Copper (transient transport component)
2—Aluminum (transient transport component)
3—Nickel (transient transport component)
4—Nickel (meniscus evaporation component)
5—Aluminum (meniscus evaporation component)
6—Copper (meniscus evaporation component)

Dashed lines represent cases where the entire residual macrolayer is washed away at the end of each period.

Solid lines represent cases where the entire residual macrolayer remains intact at the end of each period.

Fig. 6. Components of total heat transfer for different cases of Table I.

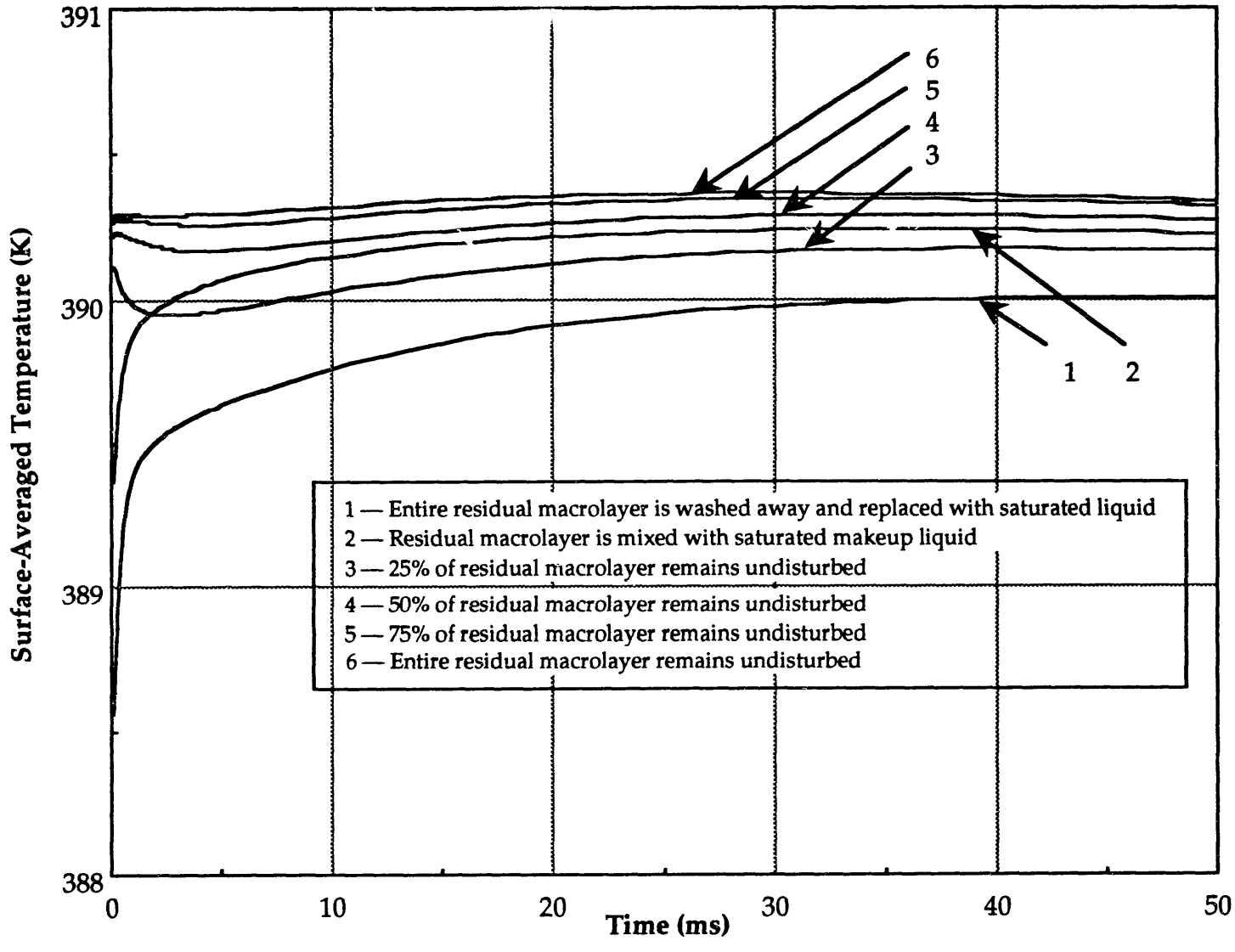

Fig. 7. Variation of surface-averaged temperature during converged hovering period (results shown for copper heater).

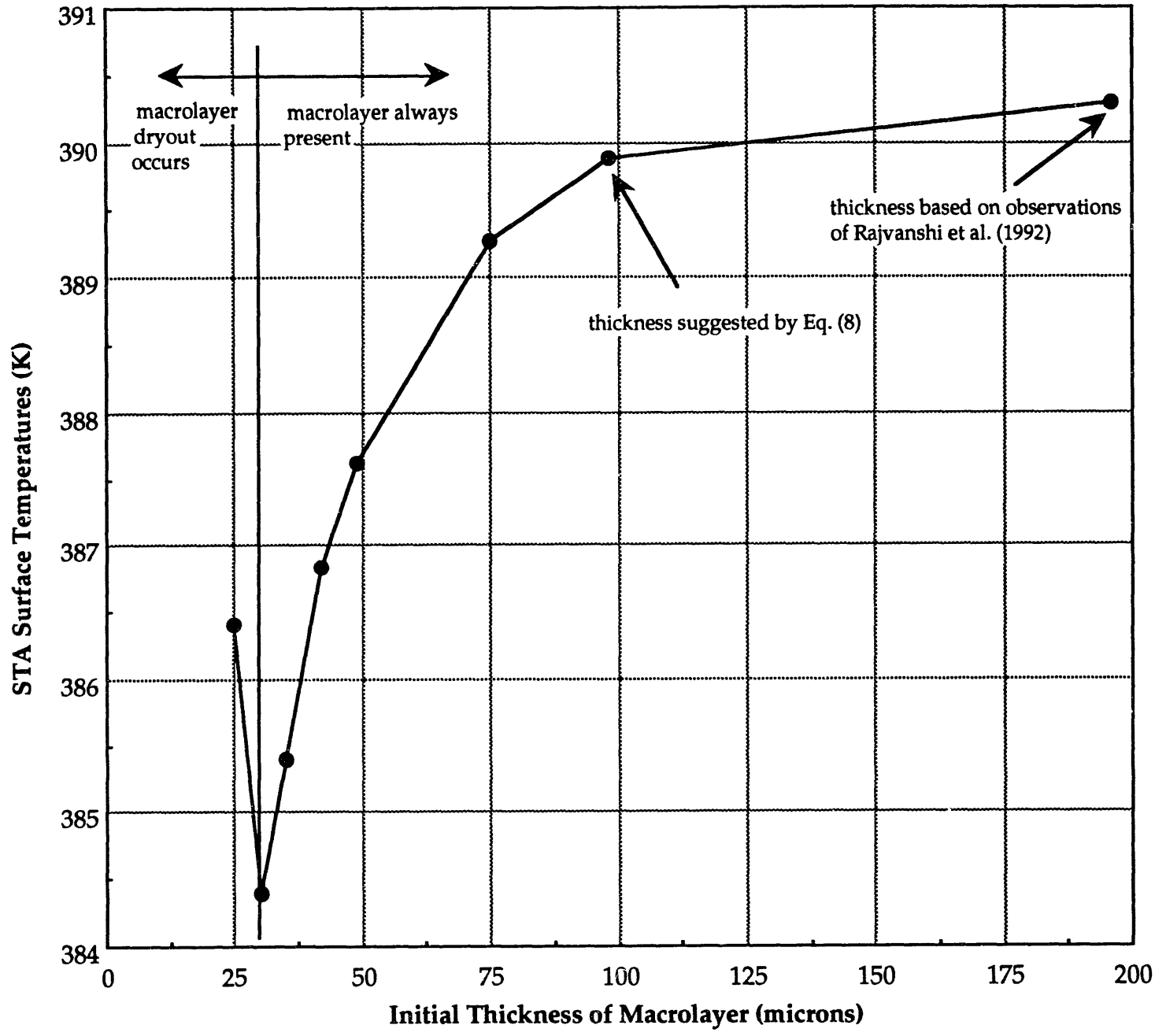

Fig. 8. Effect of initial macrolayer thickness on the boiling curve.

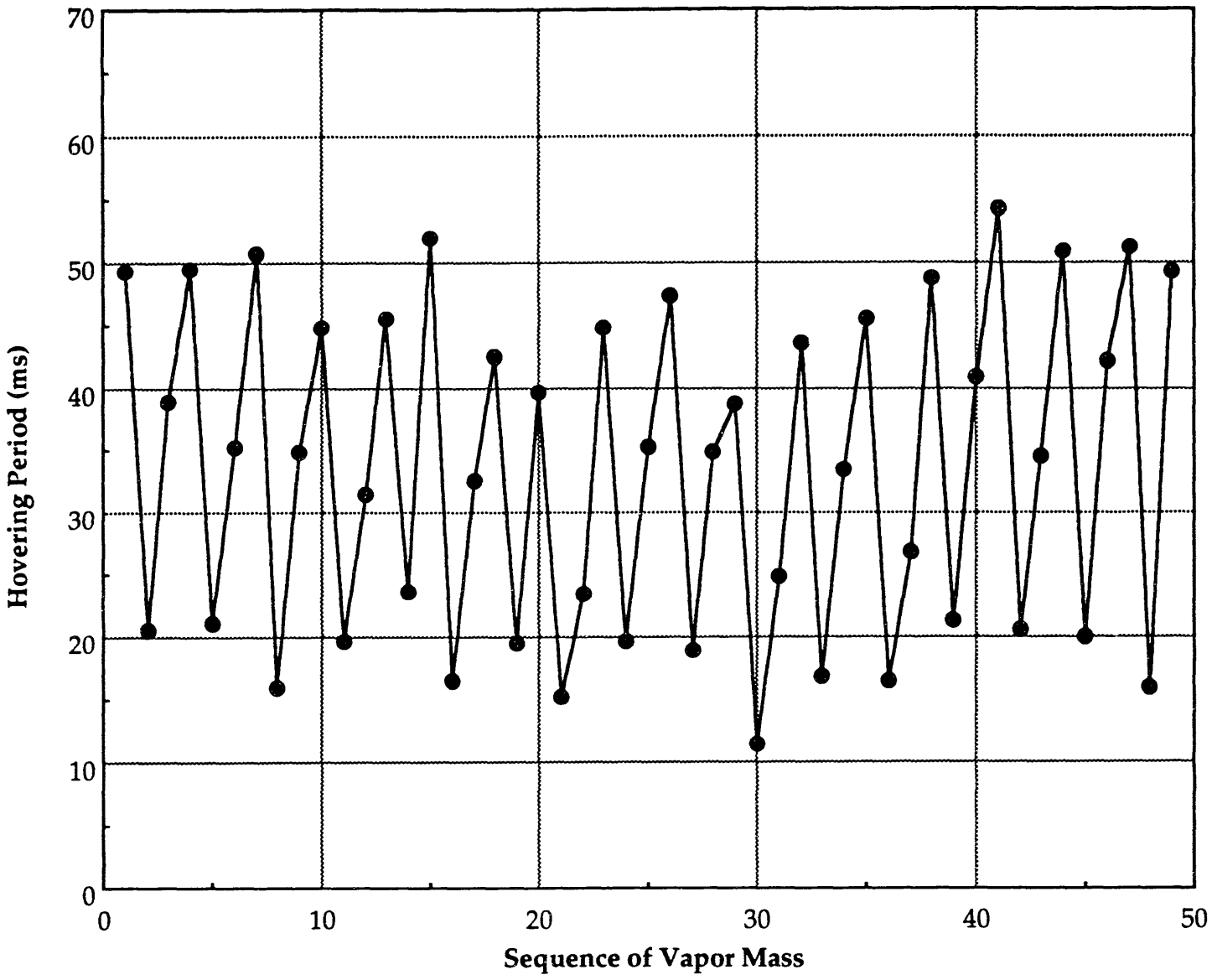

Fig. 9. Data of Katto and Yokoya (1976) showing sequence of multiple hovering periods in nucleate boiling.

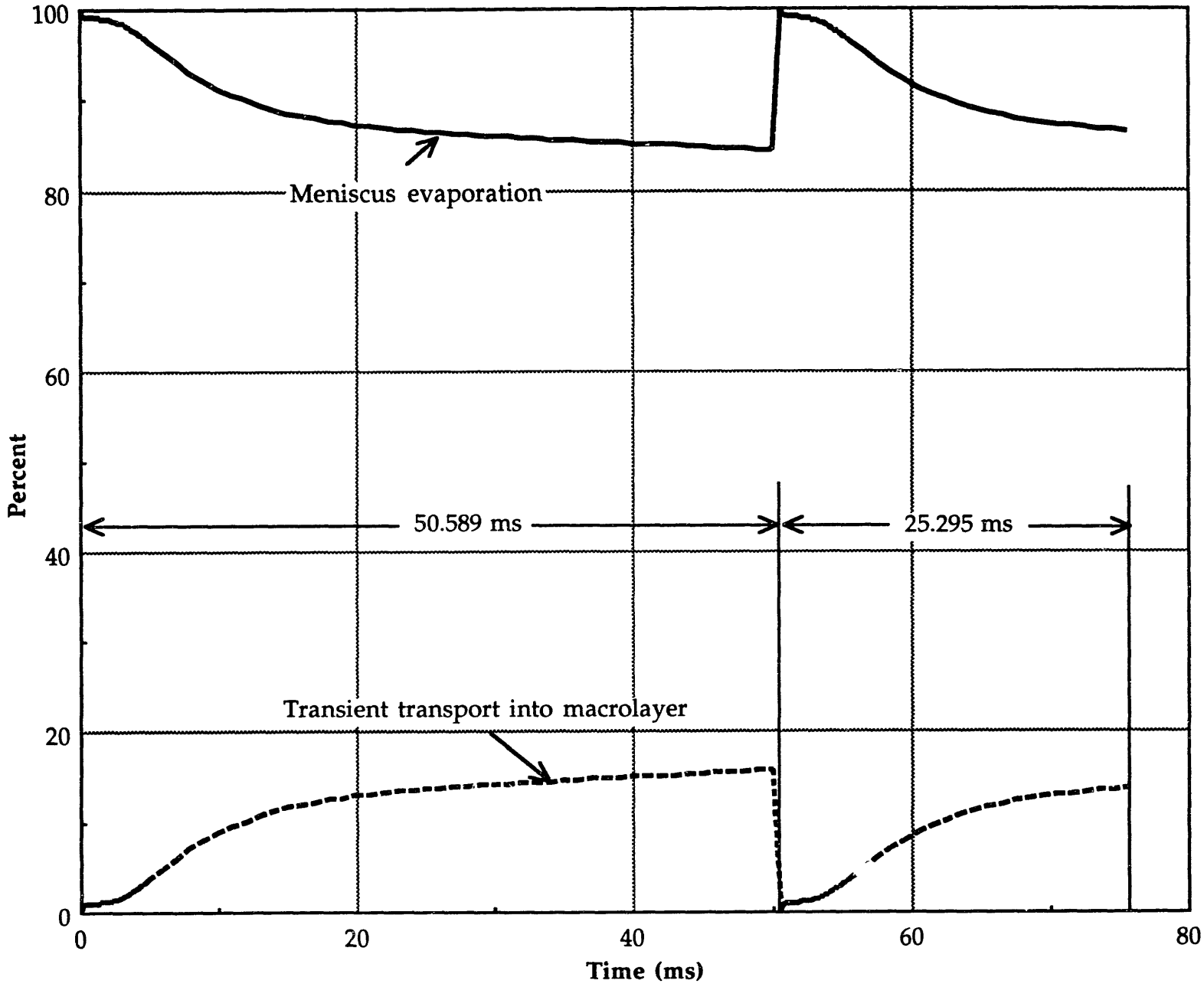

Fig. 10. Contribution of transient transport and meniscus evaporation to overall heat transfer.

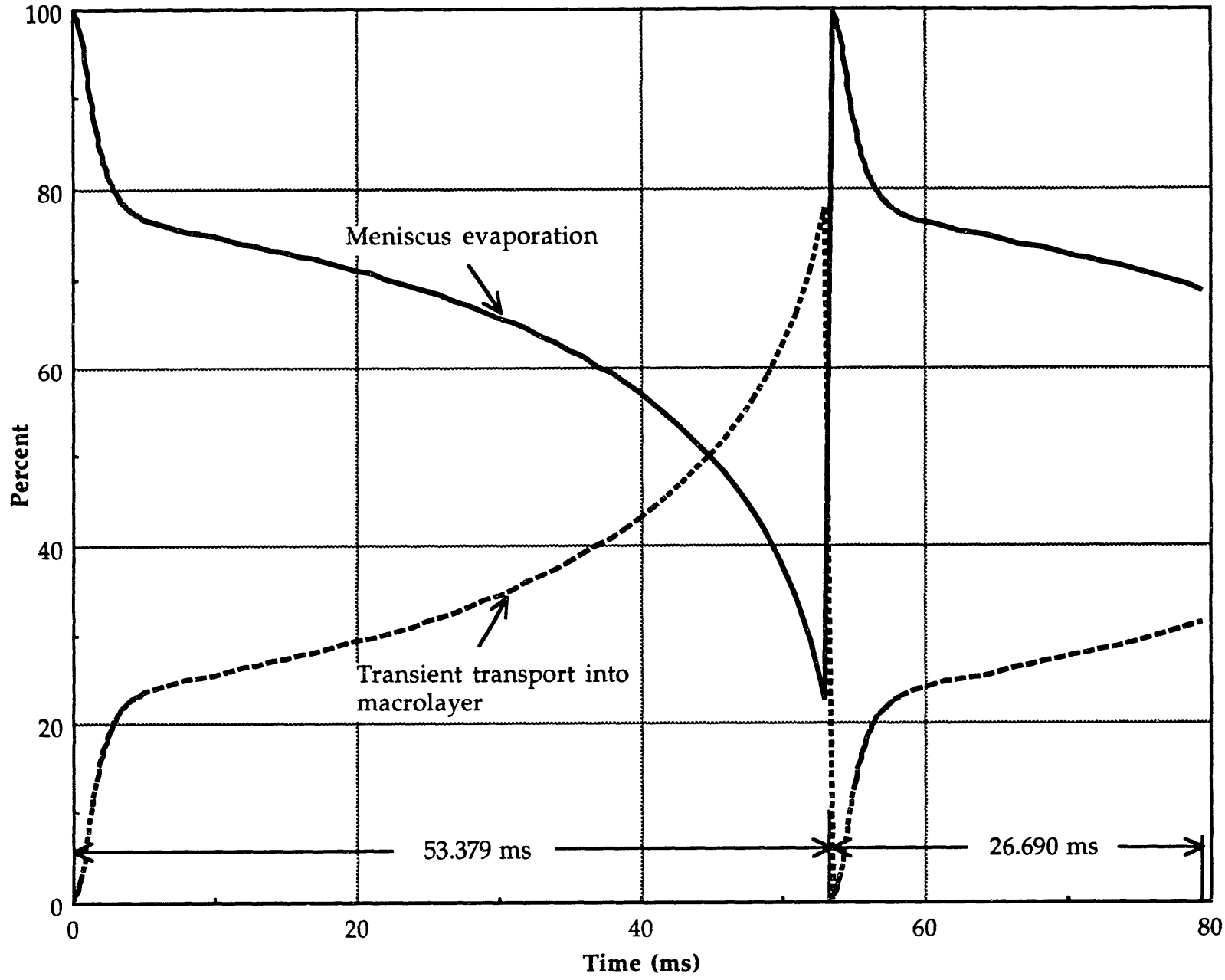

Fig. 11. Contribution of transient transport and meniscus evaporation to overall heat transfer.

DATE
FILMED
10/13/93
END